



Universiteit  
Leiden  
The Netherlands

## **Breast cancer genomes from CHEK2 c.1100delC mutation carriers lack somatic TP53 mutations and display a unique structural variant size distribution profile**

Smid, M.; Schmidt, M.K.; Smissen, W.J.C. van der; Ruigrok-Ritstier, K.; Schreurs, M.A.C.; Cornelissen, S.; ... ; Hollestelle, A.

### **Citation**

Smid, M., Schmidt, M. K., Smissen, W. J. C. van der, Ruigrok-Ritstier, K., Schreurs, M. A. C., Cornelissen, S., ... Hollestelle, A. (2023). Breast cancer genomes from CHEK2 c.1100delC mutation carriers lack somatic TP53 mutations and display a unique structural variant size distribution profile. *Breast Cancer Research*, 25(1).  
doi:10.1186/s13058-023-01653-0

Version: Publisher's Version  
License: [Creative Commons CC BY 4.0 license](#)  
Downloaded from: <https://hdl.handle.net/1887/3720616>

**Note:** To cite this publication please use the final published version (if applicable).

RESEARCH

Open Access



# Breast cancer genomes from *CHEK2* c.1100delC mutation carriers lack somatic *TP53* mutations and display a unique structural variant size distribution profile

Marcel Smid<sup>1</sup>, Marjanka K. Schmidt<sup>2,3</sup>, Wendy J. C. Prager-van der Smissen<sup>1</sup>, Kirsten Ruigrok-Ritstier<sup>1</sup>, Maartje A. C. Schreurs<sup>1,2</sup>, Sten Cornelissen<sup>4</sup>, Aida Marsal Garcia<sup>1</sup>, Annegien Broeks<sup>4</sup>, A. Mieke Timmermans<sup>1</sup>, Anita M. A. C. Trapman-Jansen<sup>1</sup>, J. Margriet Collée<sup>5</sup>, Muriel A. Adank<sup>6</sup>, Maartje J. Hooning<sup>1</sup>, John W. M. Martens<sup>1</sup> and Antoinette Hollestelle<sup>1\*</sup>

## Abstract

**Background** *CHEK2* c.1100delC was the first moderate-risk breast cancer (BC) susceptibility allele discovered. Despite several genomic, transcriptomic and functional studies, however, it is still unclear how exactly *CHEK2* c.1100delC promotes tumorigenesis. Since the mutational landscape of a tumor reflects the processes that have operated on its development, the aim of this study was to uncover the somatic genomic landscape of *CHEK2*-associated BC.

**Methods** We sequenced primary BC (pBC) and normal genomes of 20 *CHEK2* c.1100delC mutation carriers as well as their pBC transcriptomes. Including pre-existing cohorts, we exhaustively compared *CHEK2* pBC genomes to those from *BRCA1/2* mutation carriers, those that displayed homologous recombination deficiency (HRD) and ER– and ER+ pBCs, totaling to 574 pBC genomes. Findings were validated in 517 metastatic BC genomes subdivided into the same subgroups. Transcriptome data from 168 ER+ pBCs were used to derive a *TP53*-mutant gene expression signature and perform cluster analysis with *CHEK2* BC transcriptomes. Finally, clinical outcome of *CHEK2* c.1100delC carriers was compared with BC patients displaying somatic *TP53* mutations in two well-described retrospective cohorts totaling to 942 independent pBC cases.

**Results** BC genomes from *CHEK2* mutation carriers were most similar to ER+ BC genomes and least similar to those of *BRCA1/2* mutation carriers in terms of tumor mutational burden as well as mutational signatures. Moreover, *CHEK2* BC genomes did not show any evidence of HRD. Somatic *TP53* mutation frequency and the size distribution of structural variants (SVs), however, were different compared to ER+ BC. Interestingly, BC genomes with bi-allelic *CHEK2* inactivation lacked somatic *TP53* mutations and transcriptomic analysis indicated a shared biology with *TP53* mutant BC. Moreover, *CHEK2* BC genomes had an increased frequency of > 1 Mb deletions, inversions and tandem duplications with peaks at specific sizes. The high chromothripsis frequency among *CHEK2* BC genomes appeared, however, not associated with this unique SV size distribution profile.

\*Correspondence:

Antoinette Hollestelle

a.hollestelle@erasmusmc.nl

Full list of author information is available at the end of the article



© The Author(s) 2023. **Open Access** This article is licensed under a Creative Commons Attribution 4.0 International License, which permits use, sharing, adaptation, distribution and reproduction in any medium or format, as long as you give appropriate credit to the original author(s) and the source, provide a link to the Creative Commons licence, and indicate if changes were made. The images or other third party material in this article are included in the article's Creative Commons licence, unless indicated otherwise in a credit line to the material. If material is not included in the article's Creative Commons licence and your intended use is not permitted by statutory regulation or exceeds the permitted use, you will need to obtain permission directly from the copyright holder. To view a copy of this licence, visit <http://creativecommons.org/licenses/by/4.0/>. The Creative Commons Public Domain Dedication waiver (<http://creativecommons.org/publicdomain/zero/1.0/>) applies to the data made available in this article, unless otherwise stated in a credit line to the data.

**Conclusions** CHEK2 BC genomes are most similar to ER+ BC genomes, but display unique features that may further unravel CHEK2-driven tumorigenesis. Increased insight into this mechanism could explain the shorter survival of CHEK2 mutation carriers that is likely driven by intrinsic tumor aggressiveness rather than endocrine resistance.

**Keywords** CHEK2, Whole-genome sequencing, Somatic cancer genome, Mutational landscape, TP53 mutation, Structural variation, Size distribution, Chromothripsis, Whole-genome duplication, Breast cancer

## Background

The *CHEK2* c.1100delC mutation, leading to premature translation termination, was discovered to be the first moderate-risk breast cancer (BC) susceptibility allele in 2002 [1, 2]. Women who carry this germline mutation have a 2.3-fold increased risk to develop BC during their life time compared with the general population [3, 4]. BCs from *CHEK2* mutation carriers are mostly of the luminal/ER+ subtype and are diagnosed at a younger age than sporadic BCs (median age of 50 vs 60 years) [5–8]. Furthermore, BC patients carrying the c.1100delC mutation have increased risk of developing a contralateral BC and a worse survival compared to sporadic BC patients although resistance to either endocrine or chemotherapy does not appear to play a role herein [5, 8–12]. To provide tailored prevention and treatment strategies for *CHEK2* mutation carriers, it is important to unravel the biological mechanism that *CHEK2* c.1100delC exploits to drive tumorigenesis.

Similar to BRCA1 and BRCA2, CHEK2 operates in the DNA damage response (DDR) pathway. Once activated, CHEK2 is able to phosphorylate more than 20 different effector proteins involved in DNA repair, cell cycle regulation, TP53 signaling and apoptosis (e.g., BRCA1, CDC25A, TP53, and PML) [13]. Considering the central role of CHEK2 in these pathways and the merely moderate BC risk the c.1100delC mutation confers, many of its functions must be redundant in mammary epithelial cells in which CHEK2-associated BCs arise.

Functional studies and mouse models have produced conflicting results [14–18]. One important reason for this is likely the use of either non-human model systems or non-mammary epithelial cell types. Considering the latter, hormonal factors seem to play an important role in the development of BC in women and mice carrying the c.1100delC mutation, since the vast majority of BCs in women is of the luminal/ER+ subtype [6, 7] and *Chk2* c.1100delC knock-in mice developed tumors preferentially in females [18].

In addition, results from gene expression and copy number (CN) profiling studies on CHEK2-associated BCs have also not provided significant clues regarding CHEK2-driven tumorigenesis [7, 19, 20]. In this respect, next-generation sequencing technology has provided much insight into the mutational processes that operate

during tumorigenesis in recent years. For example, mutational profiling has identified the APOBEC-catalyzed cytidine deamination to be a major source of mutation in cancer [21]. Moreover, homologous recombination repair deficiency (HRD), caused by loss of BRCA1 or BRCA2 function, leaves a specific genomic imprint on the DNA characterized by two single base substitution (SBS) signatures (SBS3 and SBS8), one small insertion/deletion (ID) signature (ID6) and two specific structural variant (SV) signatures (SV3 for BRCA1-type cancers and SV5 for BRCA2-type cancers) [22–24]. Interestingly, BCs from women carrying truncating variants in *CHEK2* did not display a dominant HRD-related mutational signature, in contrast to BCs from *BRCA1*, *BRCA2* and *PALB2* mutation carriers, but similar to BCs from *ATM* mutation carriers [25–27]. Both studies on CHEK2- and ATM-associated BCs used exome and targeted sequencing data, limiting resolution and precluding the analyses of larger SVs.

In the current study, we have sequenced the primary tumor and normal genomes of 20 *CHEK2* c.1100delC mutation carriers as well as their tumor transcriptomes. Including pre-existing genomic data, we exhaustively compared CHEK2 primary BC (pBC) genomes to pBC genomes from *BRCA1/2* mutation carriers, pBCs that displayed HRD and ER– and ER+ pBCs, totaling to 574 pBC genomes. Findings were validated in 517 metastatic BC (mBC) genomes subdivided into the same subgroups.

## Methods

### Pre-existing genomic data

As part of the International Cancer Genome Consortium's (ICGC) effort to coordinate large-scale cancer genome studies in tumors from 50 cancer types and/or subtypes, whole-genome sequencing (WGS) data from 560 pBCs were generated [23] which is available from the European Genome-phenome Archive (accession code EGAS00001001178). Information on sample selection and clinical data from this cohort is available in the supplementary data of the original study at <https://www.nature.com/articles/nature17676>.

The Center for Personalized Cancer Treatment (CPCT), involving more than 40 Dutch hospitals, aims to provide personalized cancer treatment through WGS

of patient's mBC biopsies at Hartwig Medical Foundation (HMF). The resulting WGS and clinical data included 517 mBCs suitable for our analyses at the time of our data request (September 2019, DR-085). Inclusion criteria for CPCT were described previously [28].

### Whole-genome sequencing

*CHEK2* c.1100delC mutation carriers from which we had fresh-frozen pBC tissue as well as corresponding normal tissue or blood were identified retrospectively from the tissue banks of the Erasmus MC Cancer Institute and Netherlands Cancer Institute and their family clinics. For inclusion, BCs required a tumor percentage  $\geq 40\%$  and genomic DNA of sufficient quantity ( $\geq 500$  ng) and quality ( $A260/A280 = 1.8\text{--}2.0$  and DNA length  $\geq 10$  kb) for WGS, as did the corresponding normal material. Upfront, presence of the *CHEK2* c.1100delC mutation in tumor-normal pairs was verified with a custom-made Taqman genotyping assay (Thermo Fisher, Waltham, MA) as described elsewhere [3]. It was also verified that tumor-normal pairs were from the same individual by short tandem repeat analysis using the PowerPlex16 System (Promega, Madison, WI) before sending genomic DNA from the remaining 20 *CHEK2* c.1100delC mutation carriers to HMF (Amsterdam, the Netherlands) for WGS, subsequent genome alignment and variant calling as described previously for the CPCT cohort [28]. The resulting genomic data revealed one homozygous carrier and 19 heterozygous carriers of which eleven displayed loss and six retained the wild-type *CHEK2* allele. Two had lost the mutant allele and were excluded from all further analyses, totaling to 18 *CHEK2* pBC genomes (patient and tumor characteristics in Additional file 1: Table S1).

In addition to the above, we also selected genomic DNA from three pBC-normal pairs from the Erasmus MC Cancer Institute that were previously included in the 560 pBCs from the ICGC (*i.e.*, PD4604, PD4607 and PD13620) [23]. After WGS at HMF, these samples were also processed using the same pipeline as the *CHEK2* pBCs and CPCT mBCs to compare WGS data from HMF versus ICGC pipelines.

### Subgroups for analysis

In addition to the 18 *CHEK2* pBC genomes we generated for the current study, the ICGC pBC cohort also contained three *CHEK2* c.1100delC pBC genomes of which two displayed loss of the wild-type allele, totaling to 21 *CHEK2* pBC genomes. Four ICGC pBCs with *CHEK2* mutations other than c.1100delC were excluded from all further analyses. Analyses were performed separately for the *CHEK2* group, which contained all *CHEK2* pBCs

( $n=21$ ) and the *CHEK2*\* group, which only contained *CHEK2* pBCs with bi-allelic *CHEK2* inactivation ( $n=14$ ; Fig. 1A).

To compare *CHEK2* pBC genomes to the remaining 553 pBC genomes from ICGC [23], we considered five additional groups: 1) germline *BRCA1* or 2) *BRCA2* mutation carriers that display loss of the wild-type allele, 3) samples not in groups 1 or 2 that have an HRD phenotype, and 4) ER- and 5) ER+ samples not in groups 1-3 (numbers per subgroup detailed in Fig. 1A). Some analyses were performed with an HRD+ group in which samples of groups 1-3 were combined.

Findings from analyses on pBC subgroups were validated in the 517 mBC genomes from the CPCT cohort which was subdivided into the same seven groups mentioned above (numbers per subgroup detailed in Fig. 1A).

### Bioinformatics analyses

Tumor mutational burden (TMB) was defined as the number of somatic variants (*i.e.*, SNVs, MNVs and IDs) per million mappable bases (set at 2,858,674,661/10<sup>6</sup>) [29]. R v4.0.3 was used in conjunction with several packages for a range of analyses on the BC genomes: MutationalPatterns v3.0.1 for assigning mutational signatures [30], CHORD for classifying *BRCA1*-type HRD, *BRCA2*-type HRD and homologous recombination repair proficient (HRP) tumors [31], dndscv v0.1.0 for identifying driver genes [32], Facets v0.6.1 for detecting whole-genome duplication (WGD) [33], Shatterseek v0.4 for detecting chromothripsis [34] and kmlShape v0.9.5 for calculating the Fréchet distance (<https://CRAN.R-project.org/package=kmlShape>).

HRDetect calls (*i.e.*, HRD or HRP) for the ICGC pBCs and CPCT mBCs were publicly available [31]. For WGD, the fraction of segments that showed a major CN  $\geq 2$  was calculated per sample. Since a histogram of all sample fractions showed a clear bimodal distribution, the cut-point for calling a sample WGD was established at the lowest point between the two peaks. If Shatterseek identified at least one chromothripsis region the sample was labeled positive. SV signatures were called as previously described [29]. To compare density profiles using the Fréchet distance, we first established the baseline density profile of all samples per SV type (*i.e.*, inversions, deletions and tandem duplications (TDs)). We then used the density profile of a subgroup (*e.g.*, inversions of the *CHEK2*\* group), sampled these data 100 times with replacement (bootstrapping) and calculated the Fréchet distance of each bootstrap to the baseline profile of all samples. Lastly, the distribution of 100 distances of a subgroup was compared to the distribution of distances of another subgroup using a t-test.

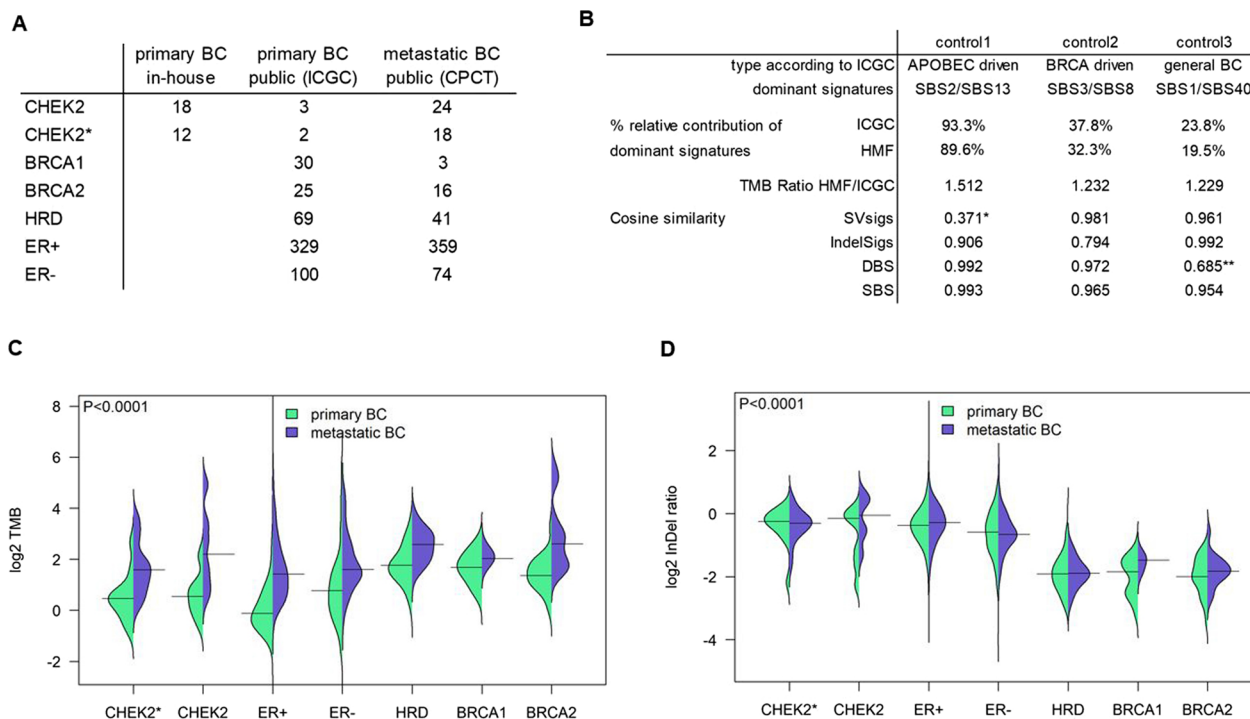


**Fig. 1** Cohorts, controls, TMB and ID ratio. **A** Numbers of samples by cohort. Four ICGC samples with *CHEK2* mutations other than c.1100delC were excluded from the dataset and subsequent analyses. **B** Results of samples analyzed on both HMF and ICGC pipelines. \*only 17 SVs and \*\*only 18 DBS for signature calling. Distributions of C TMB and D ID ratio by group. Horizontal line shows median TMB. P-values are from Kruskal–Wallis comparison of the primary BC subgroups

**RNA sequencing**

Total RNA was isolated from the same frozen tumor tissue for the 20 *CHEK2* c.1100delC mutation carriers using RNA-Bee. After clean up and DNase I treatment, 1 µg of RNA was sent to Novogene (Cambridge, UK) for Illumina RNA sequencing using a ribosomal RNA depletion method. Raw sequence files were mapped to GRCh38 using STAR v2.6.1d [35]. Sambamba v0.7.0 [36] was used to mark duplicates and index the resulting BAM files. Raw read counts for genes were obtained with featureCounts v1.6.3 [37] and normalized using GeTMM [38]. RNA sequencing data from the ICGC cohort was processed similarly [39], merged with the RNA sequencing data of the *CHEK2* cohort and adjusted for batch effects using ComBat [40]. Linear regression models were used to extract differentially expressed genes between groups. Hierarchical clustering of samples was achieved by first constructing a correlation-matrix of sample vs. sample based on these differentially expressed genes.

**Clinical cohort**

The two clinical cohorts totaled to 942 independent pBC cases and could be subdivided into our previously well-described retrospective cohorts of 760 lymph-node negative treatment-naïve ER+ BC patients (prognostic

cohort) and 323 hormone-naïve ER+ BC patients treated with first-line tamoxifen for recurrent disease (predictive cohort) [41]. The complete *TP53* coding sequence from these patient’s pBCs was evaluated for genetic alterations by Sanger sequencing (primers available upon request). *CHEK2* c.1100delC status was again determined using a previously published custom-made Taqman genotyping assay (Thermo Fisher) [3]. Loss of the wild-type *CHEK2* c.1100delC allele was evaluated by deep sequencing of a 144-bp nested-PCR amplicon encompassing the *CHEK2* mutation (primers derived from Taqman genotyping assay) on an Ion Torrent PGM (Thermo Fisher) and taking tumor cell percentage into account.

**Statistics**

Categorical data were evaluated using Pearson’s  $\chi^2$  test or Fisher’s exact test (when too few expected events). For continuous variables, a Mann–Whitney or Kruskal–Wallis test was performed. For time-to-event data, the logrank test and Cox proportional hazards models were used to compare disease-free survival between groups. Overall response (*i.e.*, complete response, partial response and stable disease >6 months vs. stable disease <6 months and progressive disease) to first-line tamoxifen treatment for recurrent disease between

groups was evaluated using logistic regression analysis. Multivariable analyses included all clinicopathological variables that displayed significant associations in univariable analyses. Other tests are indicated where applicable. All statistical tests were two-sided and considered statistically significant when  $P < 0.05$ . Stata 13.0 (StataCorp, College Station, TX) and R v4.0.3 were used to perform analysis. The Hochberg procedure was used to correct  $P$ -values for multiple hypothesis testing when appropriate.

## Results

### Comparison of sequencing pipelines

The CHEK2 pBC cohort and CPCT mBC cohort were sequenced and processed by HMF, while the ICGC pBC cohort was sequenced and processed differently [23]. Existing systematic differences between the two pipelines could confound cross-cohort comparisons. Therefore, we resequenced three tumor-normal pairs from the ICGC dataset at HMF. Comparison of these pairs showed (Fig. 1B) that the HMF pipeline called more variants, reflecting the higher tumor sequence coverage by HMF (90X) versus ICGC (40X). However, the global nature and patterns of the variants, condensed in the various mutational signatures, were very comparable between the pipelines. In fact, cosine similarities between the three pairs of SBS, double base substitution (DBS), ID and SV signatures were  $> 0.90$  for 9/12 comparisons), while 2/3 comparisons with a cosine similarity  $< 0.90$  could be explained by a low number of DSBs and SVs. If an underlying systematic bias existed between the two pipelines, overall low cosine similarities would be observed. Therefore, we were confident to perform comparative analyses between the cohorts and further subgroup pBC and mBC genomes into the following seven groups: CHEK2, CHEK2\* (*i.e.*, only CHEK2 BCs with bi-allelic CHEK2 inactivation), BRCA1, BRCA2, HRD, ER- and ER+. Subgrouping is further detailed in the Methods (numbers per subgroup listed in Fig. 1A). Additional file 1: Table S2 contains an overview of genomic events in all samples.

### TMB and ID ratio

Notwithstanding the higher rate of variants called by the HMF pipeline, pBC genomes from CHEK2 mutation carriers had a lower TMB than HRD+ pBC genomes (Fig. 1C). Distributions over all groups were significantly different ( $P < 1.0 \times 10^{-4}$ ), with false discovery rate adjusted post hoc comparisons showing significantly lower median TMB for CHEK2\* (1.37) compared to BRCA1 (3.20,  $P_{\text{adj}} = 6.5 \times 10^{-3}$ ), BRCA2 (2.55,  $P_{\text{adj}} = 0.049$ ) and HRD (3.40,  $P_{\text{adj}} = 1.3 \times 10^{-3}$ ), but not compared to ER- or ER+ pBCs (1.71 and 0.92,  $P_{\text{adj}} > 0.05$ ). Consistent with tumorigenic progression and treatment-induced

selection [29], median TMB was 2.3-fold higher in the mBC compared with the pBC cohort. However, similar differences in TMB were observed among mBC groups (Fig. 1C,  $P < 1.0 \times 10^{-4}$ ) with only CHEK2\* mBCs showing a significant lower TMB compared to HRD mBCs ( $P_{\text{adj}} = 0.013$ ) in the post hoc comparison.

The ratio of insertions over deletions (Fig. 1D) showed a similar distribution in CHEK2 pBCs compared with ER- and ER+ pBCs, while being significantly higher compared to BRCA1, BRCA2 and HRD pBCs ( $P < 1.0 \times 10^{-4}$  over all groups; FDR-adjusted post hoc comparisons  $P_{\text{adj}} = 1$  for ER+,  $P_{\text{adj}} = 0.36$  for ER-, and  $P_{\text{adj}} < 0.0001$  for HRD+ vs CHEK2\* pBC). Again, these findings were validated in the mBC cohort ( $P < 1.0 \times 10^{-4}$  over all groups; post hoc comparisons were significant for CHEK2\* vs. BRCA2 and HRD, both  $P_{\text{adj}} < 1.0 \times 10^{-4}$ ). Lastly, in contrast to the TMB, the ID ratio was not significantly increased from the primary to metastatic setting, except within ER+ BC (median of 0.77 vs. 0.82,  $P = 0.02$ ) though the effect size is very modest.

Thus, in terms of TMB and ID ratio, BC genomes of CHEK2 c.1100delC carriers are most similar to ER- and ER+ and least similar to HRD+ BC genomes.

### Mutational signatures

To reveal the mutational processes operating during breast tumorigenesis in CHEK2 c.1100delC mutation carriers, we determined the percentage relative contribution (%rc) of each of the known 67 SBS, 11 DBS, 18 ID and 6 SV signatures [23, 24]. Out of these 102 signatures, 13 SBS, 9 DSB, 13 ID and 5 SV signatures had  $\geq 5\%$  rc in  $\geq 2$  CHEK2 BC genomes (Additional file 1: Tables S3-6). For these 40 more profound signatures, we calculated the median %rc of each subgroup and constructed a condensed overview showing CHEK2\* pBCs were least similar to HRD+ and most similar to ER+ pBCs (Fig. 2A). This observation was replicated in the mBC cohort, showing CHEK2\* mBCs clustering closest to ER+ mBCs using 39/102 signatures with  $\geq 5\%$  rc in  $\geq 2$  CHEK2 mBCs (Additional file 2: Figure S1).

Since CHEK2 BCs as a group were least similar to HRD+ BCs, but CHEK2 is known as a central player in the DDR, we next evaluated whether each individual CHEK2 BC displayed HRD using classifiers CHORD and HRDetect [31, 42]. Both models use specific features in WGS data (*e.g.*, mutational signatures, but also additional characteristics) to distinguish HRD from HRP genomes. Results showed only one of the 21 CHEK2 pBCs displaying HRD, but this pBC had retained the wild-type CHEK2 allele. Again, only one of the 24 CHEK2 mBCs displayed HRD, but this CHEK2\* mBC patient carried an additional BRCA2 mutation. Finally, we also evaluated individual mutational

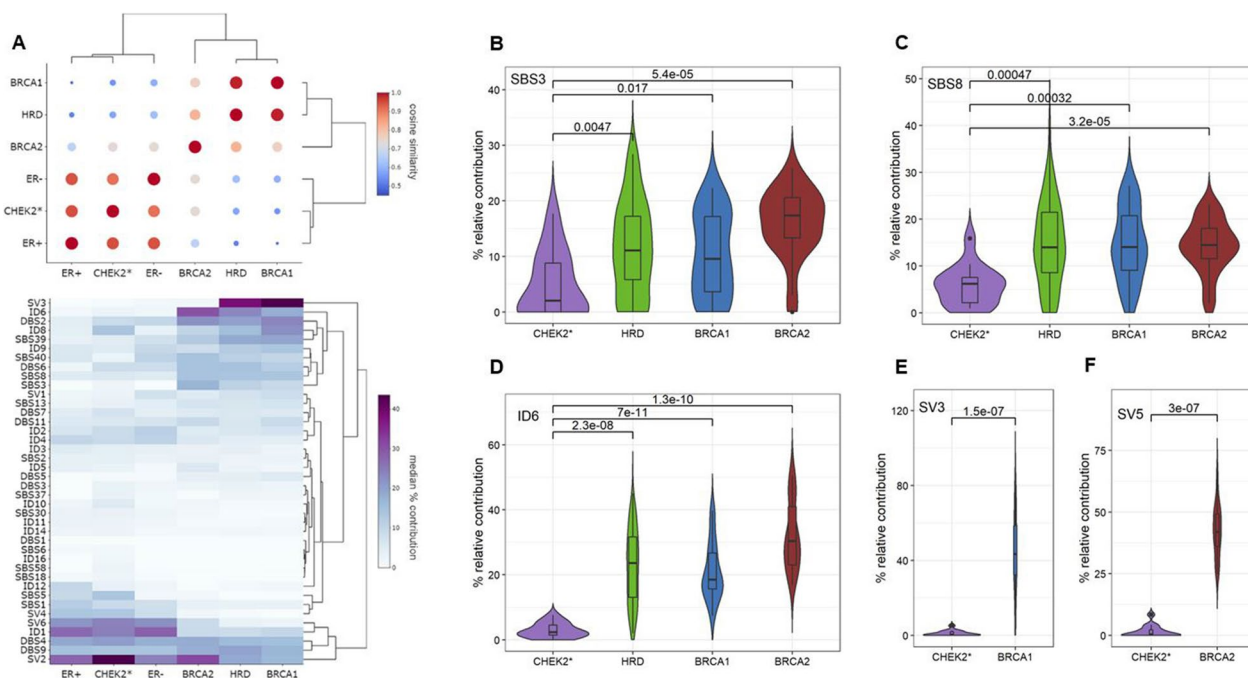


**Fig. 2** Mutational signatures in primary BC subgroups. **A** Cosine similarity coefficients (top) and hierarchical clustering (bottom) of BC subgroups based on the median % relative contribution of 40 SBS, DSB, ID and SV signatures. Percentage relative contribution of mutational signatures associated with the HRD phenotype: **B** SBS3, **C** SBS8, **D** ID6, and signatures associated with **E** BRCA1 (SV3) and **F** BRCA2 (SV5). *P*-values are based on Mann–Whitney test

signatures associated with HRD: SBS3, SBS8, ID6, SV3 and SV5 [22–24] among CHEK2 BCs as a group. However, CHEK2\* pBCs showed a significant lower median %rc of these signatures (Fig. 2B–F) compared with HRD+ pBCs, clearly indicating that CHEK2 BCs do not display the obvious mutational scars typical of HRD.

Because *CHEK2* c.1100delC is a moderate-risk allele with lower penetrance than *BRCA1* and *BRCA2* mutations, CHEK2 pBCs might have an intermediate HRD phenotype. However, comparison of SBS3, SBS8, ID6, SV3 and SV5 in CHEK2\* versus ER+ BCs did not show a significant difference in the median %rc for these signatures (Additional file 1: Tables S3–6; Additional file 2: Figure S2A). This is consistent with overall mutational signatures of CHEK2 BC genomes being most similar to ER+ BCs. Although we did find significant increases in SBS37, SBS58, ID8, ID10 and ID16 in CHEK2\* vs. ER+ pBCs (Additional file 1: Tables S3–6; Additional file 2: Figure S2B), this was not replicated among mBCs. In fact, we identified no significant differences for any of the 102 SBS, DBS, ID or SV signatures between CHEK2 and ER+ mBC genomes. Thus, CHEK2 BCs do not show any evidence for HRD and, based on mutational signatures, are indistinguishable from ER+ BC genomes.

**Somatic BC drivers**

We applied the dN/dS method to CHEK2 pBCs, but identified no CHEK2-specific BC driver genes. Therefore, we evaluated the mutation frequency of 94 known somatic BC driver genes [23]. In CHEK2 pBCs, 42 of these 94 driver genes were found mutated (combining protein-changing variants and CN alterations; Additional file 1: Table S7). Interestingly, none of the 14 CHEK2\* pBCs harbored a *TP53* mutation (*TP53* and genes > 20% mutated in CHEK2\* pBC shown in Fig. 3A), while we expected a mutation frequency similar to ER+ pBCs. Next, we compared the driver mutation frequency between CHEK2 pBCs and the other subgroups and repeated this in mBCs. Combining the results, only *CCND1* (lower frequency in HRD+;  $P_{adj}=3.6 \times 10^{-3}$  for pBC and  $P_{adj}=0.010$  for mBC) and *TP53* (higher frequency in HRD+ and ER–;  $P_{adj}=8.0 \times 10^{-7}$  and  $P_{adj}=6.6 \times 10^{-6}$  for pBC;  $P_{adj}=9.4 \times 10^{-3}$  and  $P_{adj}=6.0 \times 10^{-9}$  for mBC) were consistently significantly different after multiple testing correction (Fig. 3B, C; Additional file 1: Table S7). Intriguingly and similar to pBCs, none of the 18 CHEK2\* mBCs displayed a somatic driver mutation in *TP53* (Fig. 3C). This mutual exclusivity between bi-allelic inactivation of *CHEK2*

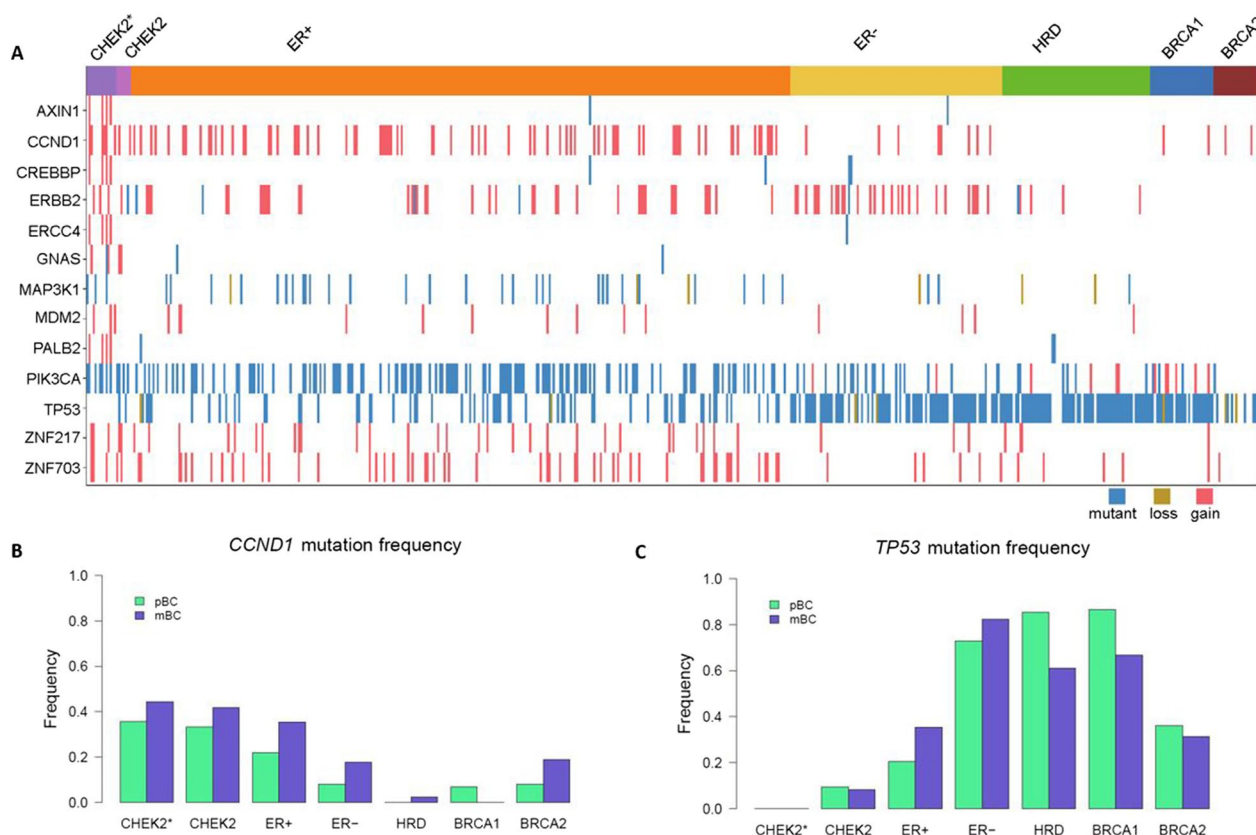


**Fig. 3** Mutation frequencies of 13 known BC driver genes among subgroups. **A** Oncoplot for *TP53* and 12 known BC driver genes with a mutation frequency > 20% in *CHEK2* pBC genomes by subgroup. wt indicates wild-type; mut, any amino-acid changing variant; del, copy number loss; amp, copy number gain. **B** Frequency of *CCND1* and **C** *TP53* mutations by subgroup

and somatic *TP53* mutations could suggest signaling of *CHEK2* c.1100delC through the *TP53* pathway.

**Transcriptomics**

If the absence of somatic *TP53* mutations from *CHEK2*\* BC genomes is a consequence of *CHEK2* c.1100delC signaling through the *TP53* pathway, this should be discernible from the *CHEK2* pBC transcriptomes (Additional file 3: Table S8). Therefore, we performed supervised clustering using 2,867 genes differentially expressed between *TP53* mutant vs wild-type ER+ pBCs from the ICGC cohort (Fig. 4A; Additional file 1: Table S9). The majority (9/14) of *CHEK2*\* pBCs clustered among the *TP53* mutant-enriched cluster ( $P=8.0 \cdot 10^{-5}$ ), while the five remaining *CHEK2*\* pBCs in the other cluster were close to the *TP53* mutant pBCs present there. Moreover, we found a 23-gene overlap between our 2,867 differently expressed genes and 31 genes from a previously published and widely used *TP53* gene signature [43]. This suggests that *CHEK2*\* pBCs indeed have shared biology with *TP53*-mutated pBCs.

Next, to identify transcriptomic features exclusive to *CHEK2*\* BCs, we extracted genes differentially expressed between *CHEK2*\* and wild-type *TP53* pBCs (Additional file 2: Figure S3A). Among these 14 genes, no pathways were enriched (DAVID) [44] or known connections were discernable (STRING database) [45]. Moreover, we did not identify any overlap with the previously published 40-gene and 862-gene signatures of Nagel et al. and Muranen et al. [7, 19]. Of the 14 genes, *ATXN7* and *CDK5RAP3* have roles in DNA repair and these were downregulated in *CHEK2*\* pBCs (Additional file 2: Figure S3B).

Thus, pBCs with bi-allelic loss of *CHEK2* share a common biology with *TP53* mutant pBCs, but no specific pathways were associated with the *CHEK2*-specific transcriptional profile itself.

**Survival and endocrine therapy resistance**

Since *CHEK2* c.1100delC mutation carriers as well as patients with somatic *TP53* mutations have been shown to have unfavorable survival [5, 8, 10, 11, 46–49], we evaluated this among our retrospective cohorts of 760

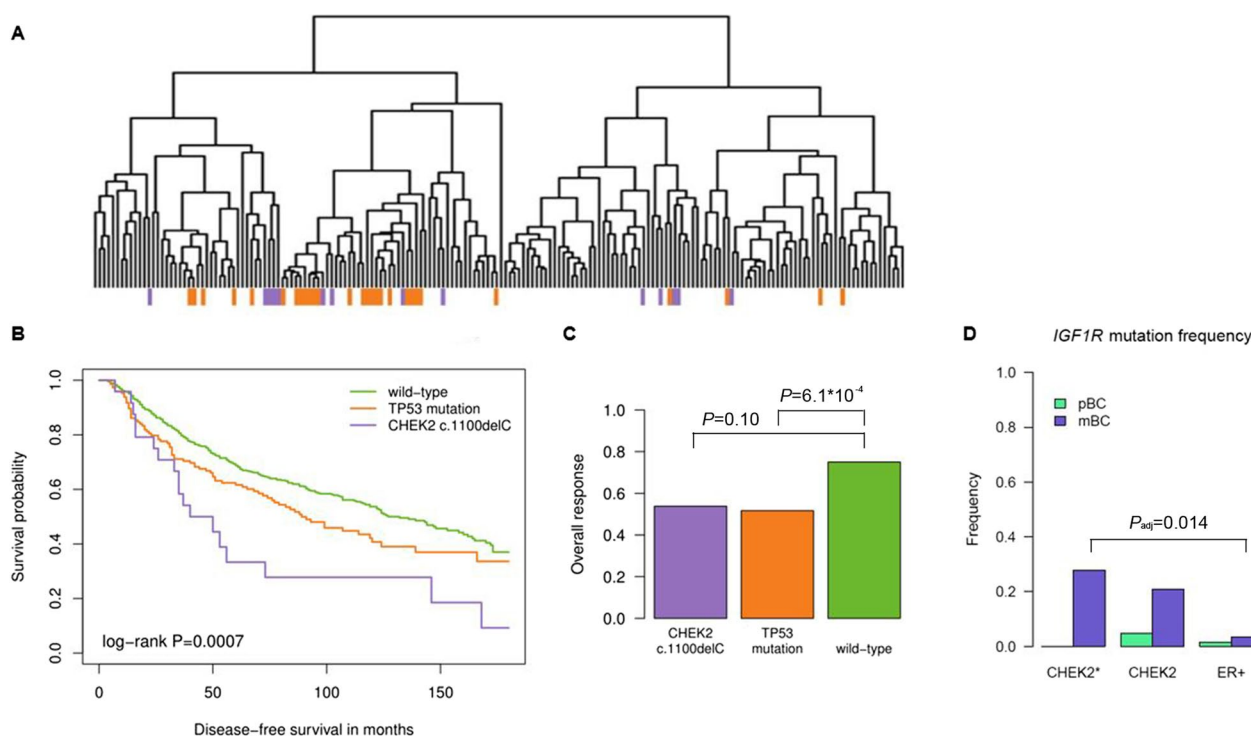


**Fig. 4** Transcriptomics, survival, tamoxifen therapy response and endocrine resistance mutations. **A** Hierarchical clustering of ER+ primary BCs (pBCs) based on 2,867 genes differentially expressed (regression model p-value < 0.05) between TP53 mutant and wild-type ER+ pBCs. CHEK2\* pBCs in purple and TP53 mutant ER+ pBCs in orange. **B** Disease-free survival and **C** overall response to first-line tamoxifen among CHEK2 c.1100delC mutation carriers, BC patients with a somatic TP53 mutation and BC patients wild-type for both alleles. **D** Mutation frequency of the endocrine resistance gene IGF1R among CHEK2 and ER+ metastatic BCs

lymph-node negative systemic treatment-naïve ER+ BC patients (prognostic cohort) and 323 hormone-naïve ER+ BC patients treated with first-line tamoxifen for recurrent disease (predictive cohort; clinicopathological variables in Additional file 1: Tables S10-11). Consistent with literature, CHEK2 c.1100delC as well as TP53 mutant BC patients had shorter disease-free survival (DFS) compared with BC patients wild-type for both alleles (CHEK2: HR=2.26, 95% CI=1.40–3.65,  $P=8.2 \times 10^{-4}$ ; TP53: HR=1.30, 95% CI=1.01–1.67,  $P=0.039$ ; Fig. 4B). After adjustment for classical prognostic factors, CHEK2 c.1100delC appeared as an independent prognostic marker for DFS (HR=2.23, 95% CI=1.07–4.61,  $P=0.031$ ; Additional file 1: Table S12). In predictive analysis, CHEK2 c.1100delC was not associated with response to tamoxifen in contrast to TP53 mutations (overall response of 53.8% and 51.7% vs. 75% in wild-type; CHEK2: OR=0.38, 95% CI=0.13–1.20,  $P=0.10$ ; TP53: OR=0.36, 95% CI=0.20–0.64,  $P=6.1 \times 10^{-4}$ ; Fig. 4C). After adjustment for classical predictive factors, somatic TP53 mutations remained independently associated with a poor response to tamoxifen treatment (OR=0.42, 95% CI=0.23–0.79,  $P=7.1 \times 10^{-3}$ ; Additional file 1: Table S13). Moreover, in the prognostic

and predictive cohort combined ( $n=942$ ;  $n=141$  BC patients in both cohorts), none of the 11 patients with bi-allelic inactivation of CHEK2 had a TP53 mutation ( $P=0.14$ ), again confirming what we observed among pBC and mBC genomes.

We also evaluated mutation frequencies of 23 genes associated with endocrine resistance in CHEK2 versus ER+ mBC genomes (Additional file 1: Table S14). Interestingly, the greatest increase in mutation frequency for CHEK2 mBC compared with pBC was observed for the IGF1R gene (0% vs. 27.8%,  $P_{\text{nom}}=0.052$ ,  $P_{\text{adj}}=1$ ). Moreover, out of these 23 genes, IGF1R was the only gene for which the mutation frequency was significantly different between CHEK2 and ER+ mBCs (27.8% vs. 3.3%,  $P_{\text{adj}}=0.014$ ) and IGF1R mutations (mostly amplifications) associated with an elevated gene expression in a subset of 127 mBCs for which we had RNAseq data ( $P=0.080$ ). However, when we combined all genes, no difference in the frequency of CHEK2 vs. ER+ mBCs with either one or multiple resistance mutations was observed (94.4% vs. 91.1%,  $P=1$ ).

Thus, we confirmed in a third independent cohort that BCs with bi-allelic loss of CHEK2 do not harbor somatic TP53 mutations and that the unfavorable survival of

CHEK2 c.1100delC carriers is likely driven by intrinsic tumor aggressiveness rather than endocrine resistance.

**WGD and chromothripsis**

Since WGD is 1.8-fold more common in BC genomes with somatic TP53 mutations [50], we also evaluated WGD among CHEK2 BC genomes. In pBCs, 143/226 (63.3%) TP53 mutant BCs had WGD compared with 62/321 (19.3%,  $P=2.2 \times 10^{-16}$ ) TP53 wild-type BCs (Fig. 5A). Interestingly, the WGD frequency of CHEK2 pBCs was in between TP53 wild-type and mutant pBCs (35.7% vs. 19.3% and 63.3%, respectively,  $P=0.17$  and  $P=0.049$ ), which fits the moderate BC risk associated with CHEK2 c.1100delC. Other subgroups, including only TP53 wild-type pBCs, had lower WGD frequencies than CHEK2\* pBCs (i.e., 18.2% combined,  $P=0.15$ ), except for BRCA1 pBCs (all four showed WGD, Fig. 5A), although this was not significant. Interestingly, WGD frequency increased 1.5 to twofold in TP53 wild-type, CHEK2\*, HRD, ER+ and ER- mBCs as compared with pBCs, but not for TP53 mutant and BRCA2 mBCs (disregarding the single BRCA1 mBC). Regardless, WGD frequency of CHEK2\* mBCs was again in between TP53 wild-type and mutant mBCs (55.6% vs. 43.8% and 68.5%, respectively,  $P=0.46$  and  $P=0.30$ ; Fig. 5A).

Chromothripsis, a single catastrophic event of clustered SVs, has also been associated with TP53 mutation [51]. Unfortunately, due to low resolution, identifying chromothripsis using the publicly available CN and SV data of ICGC was not possible. In CHEK2 pBCs, however, the chromothripsis frequency was 33.3%, which increased to 44.4% in the mBCs (Fig. 5B). Also, CHEK2 mBCs more frequently displayed chromothripsis than HRD+ mBCs (44.4% vs. 11.7%,  $P=4.5 \times 10^{-3}$ ), but not compared to ER+ and ER- mBCs (44.4% vs. 36.5% and 39.2%,  $P=0.62$  and  $P=0.79$ ; Fig. 5B). Intriguingly, although chromothripsis was most frequent among CHEK2\* mBCs, we could not replicate the association

between TP53 mutations and chromothripsis in mBCs ( $P=1$ ), however chromothripsis was associated with WGD ( $P=4.6 \times 10^{-3}$ ).

Thus, both WGD and chromothripsis increased with disease progression for CHEK2\* BCs. Moreover, CHEK2\* BCs had a WGD frequency intermediate to wild-type and TP53 mutant BCs and the highest frequency of chromothripsis compared with other mBC groups.

**Structural variant size distribution**

We also interrogated SV sizes among CHEK2 pBCs and mBCs (Additional file 1: Table S15). For inversions, both ER+ and CHEK2 pBCs displayed less small (<100 kb) inversions than other groups. Larger (>100 kb) inversions, however, were seen in all groups although size distribution patterns varied among groups. Interestingly, CHEK2 pBCs displayed two specific peaks (at 5.6 and 28.2 Mb), whereas large SV sizes in ER+ pBCs were normally distributed (Fig. 6A). We evaluated differences between SV profiles more precisely by calculating the Fréchet distance (FD) of each group’s inversion profile to the inversion profile of all samples combined (i.e., the baseline). The size distribution (after 100 bootstraps) of inversions in CHEK2\* pBCs was most comparable to ER+ pBCs, but still significantly different (mean FD from baseline of 8.38 vs. 8.04,  $P=0.033$  Fig. 6D). This observation was validated in mBCs (mean FD from baseline of 6.61 vs. 4.72,  $P<2.2 \times 10^{-16}$ ; Additional file 2: Figure S4A).

Regarding deletions, HRD+ pBCs predominantly displayed deletions <500 kb in size, whereas ER+ and CHEK2 pBCs mostly displayed deletions >500 kb. Moreover, CHEK2 pBCs specifically displayed two peaks at 4.5 and 28.2 Mb, whereas ER+ pBCs displayed one broad peak with the most frequent deletion size around 8.9 Mb (Fig. 6B). Similar to inversions, the deletion size distribution was significantly different between CHEK2 and ER+ groups, both in pBCs and mBCs (pBC: mean FD from baseline of 41.66 vs. 30.47,  $P<2.2 \times 10^{-16}$  (Fig. 6E);

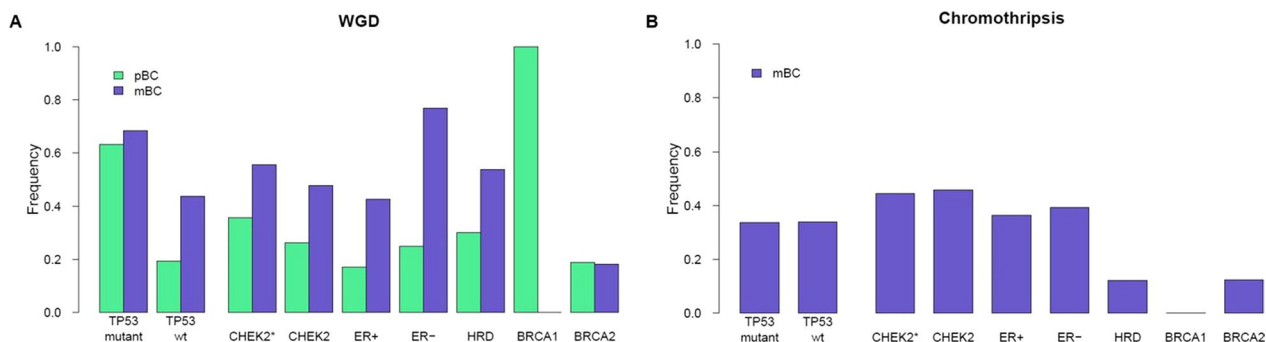


**Fig. 5** WGD and chromothripsis. **A** Frequency of WGD in primary and metastatic BC. For the subgroup frequencies, only TP53 wild-type cases were included. **B** Chromothripsis frequencies among subgroups of metastatic BC patients

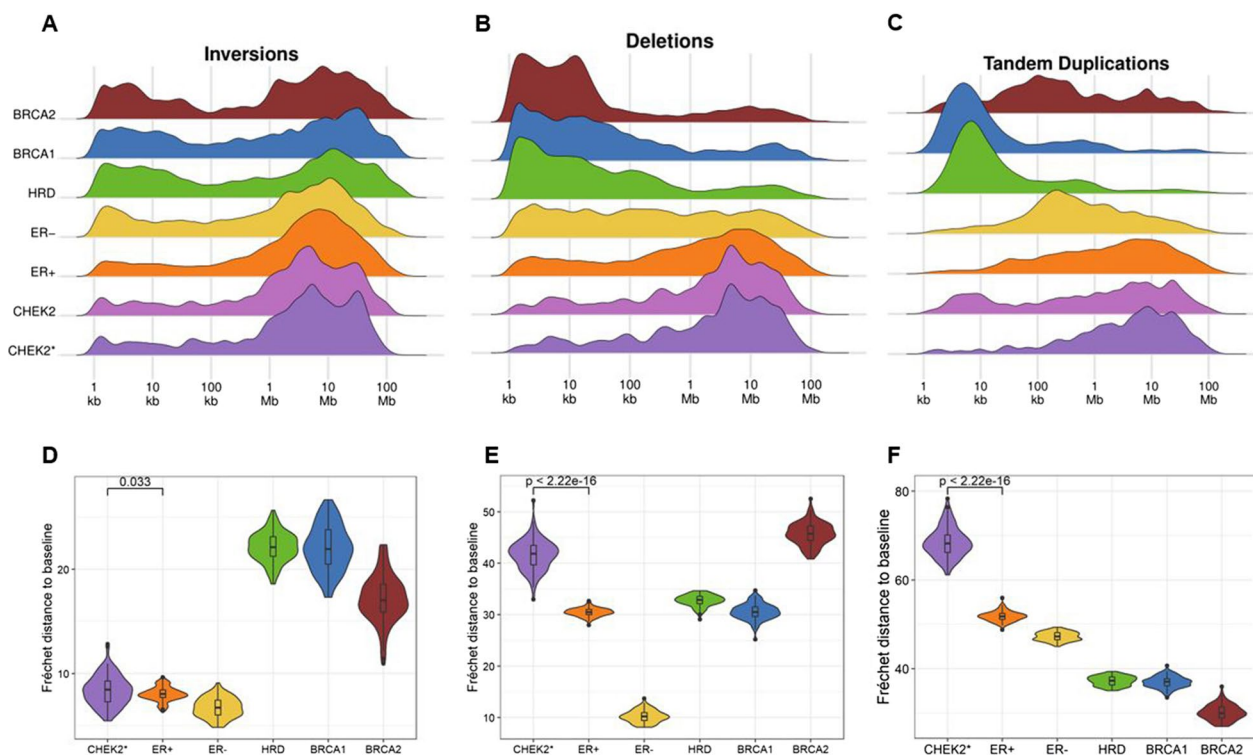


**Fig. 6** SV size distributions among primary BC subgroups. **A-C** SV size density profiles of and **D-F** Fréchet distances to baseline for inversions, deletions and tandem duplications (left to right)

mBC: 16.81 vs. 18.59,  $P=3.5 \cdot 10^{-14}$  (Additional file 2: Figure S4B). pBCs also displayed varying size distribution profiles for tandem duplications (TDs) among groups. Specifically, BRCA1 and HRD pBCs predominantly displayed smaller (< 100 kb) TDs, whereas ER- and BRCA2 pBCs mostly displayed intermediate size (50–500 kb) TDs. Larger (> 500 kb) TDs were predominantly observed for ER+ and CHEK2 pBCs. Interestingly, ER+ pBCs again displayed one broad peak, whereas CHEK2 pBCs displayed multiple peaks most prominently at 8.9 and 22.4 Mb (Fig. 6C). Consequently, also the TD size distribution was significantly different between CHEK2 and ER+ pBCs (mean FD from baseline of 68.47 vs. 51.80,  $P < 2.2 \cdot 10^{-16}$ ; Fig. 6F) and mBCs (mean FD from baseline of 33.15 vs. 23.97,  $P < 2.2 \cdot 10^{-16}$ ; Additional file 2: Figure S4C).

Taken together, CHEK2 pBCs display a unique size distribution profile of inversions, deletions and TDs, unlike any of the other pBC subgroups. Importantly, this SV size distribution profile could not be replicated by randomly subsampling SVs from ER+ pBC genomes (Additional file 2: Figure S5) indicating these findings are not a result of the smaller sample size of CHEK2 BCs. Moreover, the relatively high chromothripsis frequency in CHEK2\* mBCs did not appear to be causal for the

CHEK2 size distribution profile. Although TDs located in the CHEK2-specific peaks were more frequently located inside chromothriptic regions ( $P=8.3 \cdot 10^{-3}$ ), this was not the case for inversions and deletions ( $P=0.71$  and  $P=0.12$ , respectively), nor for TDs located in the ER+ specific peaks ( $P=0.87$ ).

### Discussion

Our interrogation of the somatic landscape of CHEK2 BCs revealed novel genomic features specific to CHEK2-driven BC. First, and in agreement with Mandelker et al., we did not observe an HRD phenotype among CHEK2 BCs [26]. Instead, CHEK2 BCs were most similar to ER+ BCs. Second, CHEK2 BC genomes that lost the wild-type *CHEK2* allele did not harbor any somatic *TP53* mutations (i.e., 0/43 in all three cohorts combined). Third, CHEK2\* BCs displayed a unique size distribution of SVs that is not simply caused by the increased chromothripsis frequency among these genomes.

There are two reasons why the latter two observations were not reported by Mandelker et al., which also represent strengths of our study. First of all, inherent to the nature of their data (from whole exome sequencing and targeted sequencing using the MSK-IMPACT panel) structural variation and related events such as

chromothripsis could not be evaluated. Second, although Mandelker et al. evaluated allelic loss at the *CHEK2* locus, they instead opted to stratify samples according to low and high-risk *CHEK2* variants. Since our cohort consisted only of BCs from c.1100delC carriers, we did not have to prioritize classification in this respect. Another strength of our study was the availability of a second cohort for validation purposes. A disadvantage of having an mBC cohort for validation, however, is that due to disease progression and/or treatment-induced selection meaningful pBC-specific associations could have been obfuscated.

Our observation that *CHEK2*\* pBCs do not harbor any somatic *TP53* mutations and have at least part of their biology in common with *TP53* mutant pBCs may not be completely surprising. Several studies in the past have found links between inactivation of *CHEK2* and *TP53* pathway signaling during tumorigenesis. However, results have often been conflicting, thus placing doubts on their validity. For example, in thymocytes from two different *Chk2*<sup>-/-</sup> mouse models *Chk2* seemed to regulate p53-dependent apoptosis [14–16], but this was not confirmed in a knock-in *Chk2* c.1100delC mouse model [17]. Moreover, before *CHEK2* c.1100delC was identified to be a moderate-risk BC susceptibility gene, it was actually a candidate gene for Li-Fraumeni syndrome [1, 2, 52, 53], which is caused by germline mutations in *TP53* [54, 55]. More recently, Boonen et al. identified *CHEK2*-dependent phosphorylation of KAP1 p.S473 to be an excellent functional read-out for pathogenicity of germline *CHEK2* variants [56]. Interestingly, KAP1 is a nuclear co-repressor that inactivates *TP53* [57]. Unfortunately, despite many links observed between *CHEK2* and *TP53*, how precisely *CHEK2* c.1100delC could promote tumorigenesis through the *TP53* pathway is still unclear. For this, functional studies in proper model systems (*i.e.*, ER+ human breast cells) are required.

Further supporting the shared biology between *CHEK2*\* and *TP53* mutant BCs is the observation that *CHEK2*\* pBCs had the highest WGD frequency among the subgroups, a feature enriched among *TP53* mutant cancers [50]. In fact, WGD frequency of *CHEK2*\* genomes was intermediate to *TP53* wild-type and mutant BCs, an observation fitting the incomplete penetrance of *CHEK2* c.1100delC. Considering the many roles of *TP53* as well as *CHEK2*, and only a subset overlapping, not all roles these proteins fulfil will be relevant for tumorigenesis. Consistent though, with the high WGD frequency among *CHEK2*\* pBCs, embryonic fibroblasts from knock-in *Chk2* c.1100delC mice showed an altered cell cycle distribution and a population of cells that are multinuclear, indicative of a cytokinesis defect [17]. It may thus be interesting to subclassify WGD-positive cancers

in those being multinucleated versus polyploid, since underlying causal mechanisms and thus players involved may be different.

Lack of somatic *TP53* mutation among *CHEK2*\* BC genomes may also be interpreted as a lack of severity of *CHEK2* c.1100delC-driven BC instead of signaling through the *TP53* pathway. However, consistent with literature [5, 8, 10, 11, 46–49], we observed that BC patients with germline *CHEK2* c.1100delC or a somatic *TP53* mutation have an unfavorable clinical outcome compared to wild-type patients. In fact, we here show that *CHEK2* c.1100delC is an independent prognostic factor, whereas *TP53* mutation is an independent predictor of response to tamoxifen. This is in agreement with two previous studies showing the efficacy of chemotherapy or endocrine therapy is unlikely to account for the unfavorable survival of *CHEK2* mutation carriers [11, 12]. However, considering the small group of *CHEK2* mutation carriers in the predictive cohort ( $n=13$ ) and the similar overall response rates in *CHEK2* mutation carriers and patients with *TP53* mutations, power could have been an issue in this analysis. If proven irreproducible, *IGF1R* could be an endocrine resistance gene to investigate further since *IGF1R* overexpression has been associated with poor outcome and resistance to conventional BC therapies [58].

Another key finding from our analyses was that *CHEK2* BCs display a unique size distribution of SVs, most similar to, but significantly different from ER+ BCs. Considering previous reports associating genes with a specific SV size distribution, size distribution profiles can also be considered biological scars arising from specific mutational events. For example, combined inactivation of *TP53* and *BRCA1* produced TDs with an average length of 11 kb, while CCNE1 pathway activation and *CDK12* mutations generated TDs with an average length of 231 kb and 1.7 Mb, respectively [59]. In addition, deletions in metastatic colorectal cancers were predominantly 10 kb to 1 Mb in size and frequently located in common fragile sites. Further analyses of breakpoints and localization of these deletions suggested transcription-dependent double-fork failure as an origin [60]. Therefore, unravelling the underlying mechanism that generates the *CHEK2*-specific SV size distribution profile would be an important aspect of understanding how *CHEK2* c.1100delC promotes breast tumorigenesis. Despite the high chromothripsis frequency among *CHEK2*\* BCs, chromothripsis did not appear to be the (sole) driver of the *CHEK2*-specific SV size distribution profile. Also, a mechanistic overlap with previously published size distribution patterns is not evident [59, 60].

*CHEK2*\* BCs were most similar to ER+ BCs, even indistinguishable in some aspects, suggesting overlapping tumor evolution. Still, *CHEK2* c.1100delC carriers

have a shorter survival and intrinsic tumor aggressiveness plays a role. To provide efficacious anti-cancer treatment and chemoprevention for these women, we need to identify the Achilles' heel for CHEK2-driven tumorigenesis. We and others have by now firmly established that CHEK2 BCs do not display HRD and thus *CHEK2* mutation carriers will not benefit from PARP inhibitor therapy [26, 61–63]. Moreover, because of the relatively low TMB we observed among CHEK2 BCs, these women are also not likely to benefit from immune checkpoint inhibitor therapy, but clinical trials investigating this are needed. The CHEK2-specific genomic features we identified here should therefore be further interrogated *in silico* as well as propel further functional experiments to finally unravel the mechanism of CHEK2-driven tumorigenesis, thereby paving the way for personalized medicine for *CHEK2* mutation carriers.

## Conclusions

CHEK2 BC genomes were most similar to non-HRD, ER+ BC genomes in terms of TMB, ID ratio as well as the various mutational signatures, yet they display a worse prognosis likely originating from an increased intrinsic tumor aggressiveness. Unfortunately, considering HRD status as well as TMB, *CHEK2* mutation carriers are not likely to benefit from either PARP inhibitors or immune checkpoint inhibitors. Importantly, CHEK2 BC\* genomes did not harbor somatic *TP53* mutations and displayed similar biology as *TP53* mutant BCs. Moreover, CHEK2\* BC genomes display a unique size distribution of SVs that is not simply caused by the increased chromothripsis frequency among these genomes. These findings provide novel clues for unraveling the mechanisms of CHEK2-driven tumorigenesis.

## Abbreviations

APOBEC	Apolipoprotein B mRNA editing enzyme, catalytic polypeptide
ATM	Ataxia telangiectasia-mutated
BC	Breast cancer
BRCA1	Breast cancer type 1 susceptibility protein
BRCA2	Breast cancer type 2 susceptibility protein
CCND1	Cyclin D1
CCNE1	Cyclin E1
CDC25A	Cell division cycle 25 homolog A
CDK12	Cyclin-dependent kinase 12
CHEK2	Checkpoint kinase 2
CN	Copy number
CPCT	Center for Personalized Cancer Treatment
DBS	Double base substitution
DFS	Disease-free survival
DDR	DNA damage response
ER	Estrogen receptor
FD	Fréchet distance
HMF	Hartwig Medical Foundation
HR	Hazard ratio
HRD	Homologous recombination repair deficient
HRP	Homologous recombination repair proficient

ICGC	International Cancer Genome Consortium
IGF1R	Insulin growth factor 1 receptor
ID	Insertion/deletion
Kb	Kilo base
Mb	Mega base
mBC	Metastatic breast cancer
MNV	Multi nucleotide variant
OR	Odds ratio
PALB2	Partner and localizer of BRCA2
PARP	Poly ADP ribose polymerase
pBC	Primary breast cancer
PML	Promyelocytic leukemia protein
SBS	Single base substitution
SNV	Single nucleotide variant
SV	Structural variant
TD	Tandem duplication
TMB	Tumor mutational burden
TP53	Tumor protein p53
WGD	Whole-genome duplication
WGS	Whole-genome sequencing

## Supplementary Information

The online version contains supplementary material available at <https://doi.org/10.1186/s13058-023-01653-0>.

**Additional file 1: Table S1.** Characteristics of breast cancers from CHEK2 c.1100delC mutation carriers. **Table S2.** Number of variants, TMB, ID ratio, TP53 status, WGD, chromothripsis and percentage relative contribution of SBS, DSB, ID and SV signatures for primary and metastatic breast cancer genomes. **Table S3.** Relative contribution of major single base substitution signatures in primary and metastatic breast cancer genomes. **Table S4.** Relative contribution of major doublet base substitution signatures in primary and metastatic breast cancer genomes. **Table S5.** Relative contribution of major small indel signatures in primary and metastatic breast cancer genomes. **Table S6.** Relative contribution of 6 known structural variant signatures in CHEK2 versus HRD, ER– and ER+ primary breast cancer genomes. **Table S7.** Somatic driver gene mutation frequencies in primary and metastatic breast cancer genomes. **Table S9.** Genes differentially expressed between TP53 mutant and wild-type pBCs. **Table S10.** Clinicopathological variables of 760 ER+ lymph node negative treatment-naïve breast cancer patients. **Table S11.** Clinicopathological variables of 323 hormone-naïve ER+ breast cancer patients treated with first-line tamoxifen for recurrent disease. **Table S12.** Univariable and multivariable Cox regression analysis of disease-free survival in 760 ER+ lymph node negative treatment-naïve breast cancer patients. **Table S13.** Univariable and multivariable logistic regression analysis of overall response in 323 hormone-naïve ER+ breast cancer patients treated with first-line tamoxifen for recurrent disease. **Table S14.** Endocrine therapy resistance gene mutation frequencies in metastatic breast cancer genomes. **Table S15.** Sizes of structural variant types in primary and metastatic breast cancer genomes.

**Additional file 2: Figure S1.** Mutational signatures among metastatic BC genomes. **Figure S2.** Relative contribution of mutational signatures in CHEK2\* and ER+ pBC genomes. **Figure S3.** Genes differentially expressed between CHEK2\* versus TP53 wild-type ER+ pBCs. **Figure S4.** Distribution of Fréchet distances among the subgroups of mBC genomes. **Figure S5.** Subsampling SVs from ER+ pBC genomes.

**Additional file 3: Table S8.** RNA sequencing log<sub>2</sub> GeTMM values from CHEK2 pBCs.

## Acknowledgements

We would like to acknowledge the NKI-AVL Core Facility Molecular Pathology & Biobanking (CFMPB) for supplying NKI-AVL Biobank material and/or lab support. The authors also thank Hartwig Medical Foundation for additional data generation and processing as well as Ronald van Marion and Dr. Ron Smits for technical assistance and Dr. Rob F.M. Wolthuis for fruitful discussions.

### Author contributions

JWMM and AH contributed to the conceptualization. MKS, MAA, MJH and AH provided funding. KR, SC, AB, WJCP, AMT, AMACT, MACS and JMC contributed to sample collection, processing, quality control, analyses and preparation for whole-genome sequencing. WJCP and AMG performed mutation analyses in the clinical cohort. MS and AH contributed to the bioinformatics and statistical analysis. AH supervised the study. MS and AH wrote the manuscript with contributions from all authors. All authors read and approved the final manuscript.

### Funding

This work was supported by a grant from the Dutch Cancer Society (KWF 10758/2016-2).

### Availability of data and materials

Somatic genomic features and RNA sequencing data from CHEK2 pBCs generated for this study are included in this published article and its supplementary information files. The previously published pBC genome dataset generated by the ICGC [23] is available in the European Genome-phenome Archive under accession code EGAS00001001178. The pre-existing mBC genome dataset was generated by the CPCT [29] and obtained from HMF under data request DR-085.

### Declarations

#### Ethics approval and consent to participate

This study was approved by the Medical Ethical Committees of the Erasmus University Medical Centre (MEC 02.953 and MEC 11.226) and the Netherlands Cancer Institute (CFMPB652). All retrospective medical data and/or biospecimen studies at both institutes have been executed pursuant to Dutch legislation and international standards. Prior to 25 May 2018, national legislation on data protection applied, as well as the International Guideline on Good Clinical Practice. From 25 May 2018, we also adhere to the GDPR. Within this framework, patients are informed and have always had the opportunity to object or actively consent to the (continued) use of their personal data and biospecimens in research. Hence, the procedures comply both with (inter-) national legislative and ethical standards.

#### Consent for publication

Not applicable.

#### Competing interests

The authors declare no potential competing interests.

#### Author details

<sup>1</sup>Department of Medical Oncology, Erasmus MC Cancer Institute, Rotterdam, The Netherlands. <sup>2</sup>Division of Molecular Pathology, The Netherlands Cancer Institute - Antoni van Leeuwenhoek Hospital, Amsterdam, The Netherlands. <sup>3</sup>Department of Clinical Genetics, Leiden University Medical Center, Leiden, The Netherlands. <sup>4</sup>Core Facility Molecular Pathology & Biobanking, The Netherlands Cancer Institute - Antoni van Leeuwenhoek Hospital, Amsterdam, The Netherlands. <sup>5</sup>Department of Clinical Genetics, Erasmus University Medical Center, Rotterdam, The Netherlands. <sup>6</sup>Family Cancer Clinic, The Netherlands Cancer Institute - Antoni van Leeuwenhoek Hospital, Amsterdam, The Netherlands.

Received: 13 March 2023 Accepted: 2 May 2023

Published online: 09 May 2023

### References

- Meijers-Heijboer H, van den Ouweland A, Klijn J, Wasielewski M, de Snoo A, Oldenburg R, et al. Low-penetrance susceptibility to breast cancer due to CHEK2(\*)1100delC in noncarriers of BRCA1 or BRCA2 mutations. *Nat Genet.* 2002;31:55–9.
- Vahteristo P, Bartkova J, Eerola H, Syrjakoski K, Ojala S, Kilpivaara O, et al. A CHEK2 genetic variant contributing to a substantial fraction of familial breast cancer. *Am J Hum Genet.* 2002;71:432–8.
- CHEK2 Breast Cancer Case-Control Consortium. CHEK2\*1100delC and susceptibility to breast cancer: a collaborative analysis involving 10,860 breast cancer cases and 9,065 controls from 10 studies. *Am J Hum Genet.* 2004;74:1175–82.
- Schmidt MK, Hogervorst F, van Hien R, Cornelissen S, Broeks A, Adank MA, et al. Age- and tumor subtype-specific breast cancer risk estimates for CHEK2\*1100delC carriers. *J Clin Oncol.* 2016;34:2750–60.
- de Bock GH, Schutte M, Krol-Warmerdam EM, Seynaeve C, Blom J, Brekelmans CT, et al. Tumour characteristics and prognosis of breast cancer patients carrying the germline CHEK2\*1100delC variant. *J Med Genet.* 2004;41:731–5.
- Domagala P, Wokolorczyk D, Cybulski C, Huzarski T, Lubinski J, Domagala W. Different CHEK2 germline mutations are associated with distinct immunophenotypic molecular subtypes of breast cancer. *Breast Cancer Res Treat.* 2012;132:937–45.
- Nagel JH, Peeters JK, Smid M, Sieuwerts AM, Wasielewski M, de Weerd V, et al. Gene expression profiling assigns CHEK2 1100delC breast cancers to the luminal intrinsic subtypes. *Breast Cancer Res Treat.* 2012;132:439–48.
- Weischer M, Nordestgaard BG, Pharoah P, Bolla MK, Nevanlinna H, Van't Veer LJ, et al. CHEK2\*1100delC heterozygosity in women with breast cancer associated with early death, breast cancer-specific death, and increased risk of a second breast cancer. *J Clin Oncol.* 2012;30:4308–16.
- Broeks A, de Witte L, Nooijen A, Huseinovic A, Klijn JG, van Leeuwen FE, et al. Excess risk for contralateral breast cancer in CHEK2\*1100delC germline mutation carriers. *Breast Cancer Res Treat.* 2004;83:91–3.
- Schmidt MK, Tollenaar RA, de Kemp SR, Broeks A, Cornelisse CJ, Smit VT, et al. Breast cancer survival and tumor characteristics in premenopausal women carrying the CHEK2\*1100delC germline mutation. *J Clin Oncol.* 2007;25:64–9.
- Kriege M, Hollestelle A, Jager A, Huijts PE, Berns EM, Sieuwerts AM, et al. Survival and contralateral breast cancer in CHEK2 1100delC breast cancer patients: impact of adjuvant chemotherapy. *Br J Cancer.* 2014;111:1004–13.
- Kriege M, Jager A, Hollestelle A, Berns EM, Blom J, Meijer-van Gelder ME, et al. Sensitivity to systemic therapy for metastatic breast cancer in CHEK2 1100delC mutation carriers. *J Cancer Res Clin Oncol.* 2015;141:1879–87.
- Zannini L, Delia D, Buscemi G. Chk2 kinase in the DNA damage response and beyond. *J Mol Cell Biol.* 2014;6:442–57.
- Hirao A, Kong YY, Matsuoka S, Wakeham A, Ruland J, Yoshida H, et al. DNA damage-induced activation of p53 by the checkpoint kinase Chk2. *Science.* 2000;287:1824–7.
- Hirao A, Cheung A, Duncan G, Girard PM, Elia AJ, Wakeham A, et al. Chk2 is a tumor suppressor that regulates apoptosis in both an ataxia telangiectasia mutated (ATM)-dependent and an ATM-independent manner. *Mol Cell Biol.* 2002;22:6521–32.
- Takai H, Naka K, Okada Y, Watanabe M, Harada N, Saito S, et al. Chk2-deficient mice exhibit radioresistance and defective p53-mediated transcription. *EMBO J.* 2002;21:5195–205.
- el Bahassi M, Penner CG, Robbins SB, Tichy E, Feliciano E, Yin M, et al. The breast cancer susceptibility allele CHEK2\*1100delC promotes genomic instability in a knock-in mouse model. *Mutat Res.* 2007;616:201–9.
- el Bahassi M, Robbins SB, Yin M, Boivin GP, Kuiper R, van Steeg H, et al. Mice with the CHEK2\*1100delC SNP are predisposed to cancer with a strong gender bias. *Proc Natl Acad Sci USA.* 2009;106:17111–6.
- Muranen TA, Greco D, Fagerholm R, Kilpivaara O, Kampjarvi K, Aittomaki K, et al. Breast tumors from CHEK2 1100delC-mutation carriers: genomic landscape and clinical implications. *Breast Cancer Res.* 2011;13:R90.
- Massink MP, Kooi IE, Martens JW, Waisfisz Q, Meijers-Heijboer H. Genomic profiling of CHEK2\*1100delC-mutated breast carcinomas. *BMC Cancer.* 2015;15:877.
- Alexandrov LB, Nik-Zainal S, Wedge DC, Aparicio SA, Behjati S, Biankin AV, et al. Signatures of mutational processes in human cancer. *Nature.* 2013;500:415–21.
- Nik-Zainal S, Alexandrov LB, Wedge DC, Van Loo P, Greenman CD, Raine K, et al. Mutational processes molding the genomes of 21 breast cancers. *Cell.* 2012;149:979–93.
- Nik-Zainal S, Davies H, Staaf J, Ramakrishna M, Glodzik D, Zou X, et al. Landscape of somatic mutations in 560 breast cancer whole-genome sequences. *Nature.* 2016;534:47–54.

24. Alexandrov LB, Kim J, Haradhvala NJ, Huang MN, Tian Ng AW, Wu Y, et al. The repertoire of mutational signatures in human cancer. *Nature*. 2020;578:94–101.
25. Polak P, Kim J, Braunstein LZ, Karlic R, Haradhvala NJ, Tiao G, et al. A mutational signature reveals alterations underlying deficient homologous recombination repair in breast cancer. *Nat Genet*. 2017;49:1476–86.
26. Mandelker D, Kumar R, Pei X, Selenica P, Setton J, Arunachalam S, et al. The landscape of somatic genetic alterations in breast cancers from CHEK2 germline mutation carriers. *JNCI Cancer Spectr*. 2019;3:pkz027.
27. Weigelt B, Bi R, Kumar R, Blecua P, Mandelker DL, Geyer FC, et al. The landscape of somatic genetic alterations in breast cancers from ATM germline mutation carriers. *J Natl Cancer Inst*. 2018;110:1030–4.
28. Priestley P, Baber J, Lolkema MP, Steeghs N, de Bruijn E, Shale C, et al. Pan-cancer whole-genome analyses of metastatic solid tumours. *Nature*. 2019;575:210–6.
29. Angus L, Smid M, Wilting SM, van Riet J, Van Hoeck A, Nguyen L, et al. The genomic landscape of metastatic breast cancer highlights changes in mutation and signature frequencies. *Nat Genet*. 2019;51:1450–8.
30. Blokzijl F, Janssen R, van Boxtel R, Cuppen E. MutationalPatterns: comprehensive genome-wide analysis of mutational processes. *Genome Med*. 2018;10:33.
31. Nguyen L, J WMM, Van Hoeck A, Cuppen E. Pan-cancer landscape of homologous recombination deficiency. *Nat Commun*. 2020;11:5584.
32. Martincorena I, Raine KM, Gerstung M, Dawson KJ, Haase K, Van Loo P, et al. Universal patterns of selection in cancer and somatic tissues. *Cell*. 2017;171(1029–41): e21.
33. Shen R, Seshan VE. FACETS: allele-specific copy number and clonal heterogeneity analysis tool for high-throughput DNA sequencing. *Nucleic Acids Res*. 2016;44: e131.
34. Cortes-Ciriano I, Lee JJ, Xi R, Jain D, Jung YL, Yang L, et al. Comprehensive analysis of chromothripsis in 2,658 human cancers using whole-genome sequencing. *Nat Genet*. 2020;52:331–41.
35. Dobin A, Davis CA, Schlesinger F, Drenkow J, Zaleski C, Jha S, et al. STAR: ultrafast universal RNA-seq aligner. *Bioinformatics*. 2013;29:15–21.
36. Tarasov A, Vilella AJ, Cuppen E, Nijman IJ, Prins P. Sambamba: fast processing of NGS alignment formats. *Bioinformatics*. 2015;31:2032–4.
37. Liao Y, Smyth GK, Shi W. featureCounts: an efficient general purpose program for assigning sequence reads to genomic features. *Bioinformatics*. 2014;30:923–30.
38. Smid M, Coebergh van den Braak RRJ, van de Werken HJG, van Riet J, van Galen A, de Weerd V, et al. Gene length corrected trimmed mean of M-values (GeTMM) processing of RNA-seq data performs similarly in intersample analyses while improving intrasample comparisons. *BMC Bioinformatics*. 2018;19:236.
39. Smid M, Rodriguez-Gonzalez FG, Sieuwerts AM, Salgado R, Prager-Van der Smissen WJ, Vlugt-Daane MV, et al. Breast cancer genome and transcriptome integration implicates specific mutational signatures with immune cell infiltration. *Nat Commun*. 2016;7:12910.
40. Johnson WE, Li C, Rabinovic A. Adjusting batch effects in microarray expression data using empirical Bayes methods. *Biostatistics*. 2007;8:118–27.
41. Liu J, Sieuwerts AM, Look MP, van der Vlugt-Daane M, Meijer-van Gelder ME, Foekens JA, et al. The 29.5 kb APOBEC3B Deletion polymorphism is not associated with clinical outcome of breast cancer. *PLoS ONE*. 2016;11:e0161731.
42. Davies H, Glodzik D, Morganella S, Yates LR, Staaf J, Zou X, et al. HRDetect is a predictor of BRCA1 and BRCA2 deficiency based on mutational signatures. *Nat Med*. 2017;23:517–25.
43. Takahashi S, Moriya T, Ishida T, Shibata H, Sasano H, Ohuchi N, et al. Prediction of breast cancer prognosis by gene expression profile of TP53 status. *Cancer Sci*. 2008;99:324–32.
44. da Huang W, Sherman BT, Lempicki RA. Systematic and integrative analysis of large gene lists using DAVID bioinformatics resources. *Nat Protoc*. 2009;4:44–57.
45. Szklarczyk D, Gable AL, Nastou KC, Lyon D, Kirsch R, Pyysalo S, et al. The STRING database in 2021: customizable protein-protein networks, and functional characterization of user-uploaded gene/measurement sets. *Nucleic Acids Res*. 2021;49:D605–12.
46. Andersen TI, Holm R, Nesland JM, Heimdal KR, Ottestad L, Borresen AL. Prognostic significance of TP53 alterations in breast carcinoma. *Br J Cancer*. 1993;68:540–8.
47. Sjogren S, Inganas M, Norberg T, Lindgren A, Nordgren H, Holmberg L, et al. The p53 gene in breast cancer: prognostic value of complementary DNA sequencing versus immunohistochemistry. *J Natl Cancer Inst*. 1996;88:173–82.
48. Berns EM, Foekens JA, Vossen R, Look MP, Devilee P, Henzen-Logmans SC, et al. Complete sequencing of TP53 predicts poor response to systemic therapy of advanced breast cancer. *Cancer Res*. 2000;60:2155–62.
49. Olivier M, Langerod A, Carrieri P, Bergh J, Klaar S, Eyfjord J, et al. The clinical value of somatic TP53 gene mutations in 1,794 patients with breast cancer. *Clin Cancer Res*. 2006;12:1157–67.
50. Bielski CM, Zehir A, Penson AV, Donoghue MTA, Chatila W, Armenia J, et al. Genome doubling shapes the evolution and prognosis of advanced cancers. *Nat Genet*. 2018;50:1189–95.
51. The ICGC/TCGA Pan-Cancer Analysis of Whole Genomes Consortium. Pan-cancer analysis of whole genomes. *Nature*. 2020;578:82–93.
52. Bell DW, Varley JM, Szydlo TE, Kang DH, Wahrer DC, Shannon KE, et al. Heterozygous germ line hCHK2 mutations in Li-Fraumeni syndrome. *Science*. 1999;286:2528–31.
53. Sodha N, Houlston RS, Bullock S, Yuille MA, Chu C, Turner G, et al. Increasing evidence that germline mutations in CHEK2 do not cause Li-Fraumeni syndrome. *Hum Mutat*. 2002;20:460–2.
54. Srivastava S, Zou ZQ, Pirolo K, Blattner W, Chang EH. Germ-line transmission of a mutated p53 gene in a cancer-prone family with Li-Fraumeni syndrome. *Nature*. 1990;348:747–9.
55. Santibanez-Koref MF, Birch JM, Hartley AL, Jones PH, Craft AW, Eden T, et al. p53 germline mutations in Li-Fraumeni syndrome. *Lancet*. 1991;338:1490–1.
56. Boonen R, Wiegant WW, Celosse N, Vrolijk B, Heijl S, Kote-Jarai Z, et al. Functional analysis identifies damaging CHEK2 missense variants associated with increased cancer risk. *Cancer Res*. 2022;82:615–31.
57. Wang C, Ivanov A, Chen L, Fredericks WJ, Seto E, Rauscher FJ 3rd, et al. MDM2 interaction with nuclear corepressor KAP1 contributes to p53 inactivation. *EMBO J*. 2005;24:3279–90.
58. Zhang Y, Wester L, He J, Geiger T, Moerkens M, Siddappa R, et al. IGF1R signaling drives antiestrogen resistance through PAK2/PIX activation in luminal breast cancer. *Oncogene*. 2018;37:1869–84.
59. Menghi F, Barthel FP, Yadav V, Tang M, Ji B, Tang Z, et al. The tandem duplicator phenotype is a prevalent genome-wide cancer configuration driven by distinct gene mutations. *Cancer Cell*. 2018;34(197–210): e5.
60. Smid M, Wilting SM, Martens JWM. Lost by transcription: fork failures, elevated expression, and clinical consequences related to deletions in metastatic colorectal cancer. *Int J Mol Sci*. 2022;23.
61. Poti A, Gyergyak H, Nemeth E, Ruzs O, Toth S, Kovacshazi C, et al. Correlation of homologous recombination deficiency induced mutational signatures with sensitivity to PARP inhibitors and cytotoxic agents. *Genome Biol*. 2019;20:240.
62. Abida W, Campbell D, Patnaik A, Shapiro JD, Sautois B, Vogelzang NJ, et al. Non-BRCA DNA damage repair gene alterations and response to the PARP inhibitor rucaparib in metastatic castration-resistant prostate cancer: analysis from the phase II TRITON2 Study. *Clin Cancer Res*. 2020;26:2487–96.
63. Tung NM, Robson ME, Venz S, Santa-Maria CA, Nanda R, Marcom PK, et al. TBCRC 048: Phase II study of olaparib for metastatic breast cancer and mutations in homologous recombination-related genes. *J Clin Oncol*. 2020;38:4274–82.

## Publisher's Note

Springer Nature remains neutral with regard to jurisdictional claims in published maps and institutional affiliations.